Infrared-optical double resonance spectroscopy: A selective and sensitive tool to investigate structures of molecular clusters in the gas phase

Prashant Chandra Singh and G. Naresh Patwari*

Department of Chemistry, Indian Institute of Technology Bombay, Powai, Mumbai 400 076, India

A spectrometer to investigate molecules and molecular clusters in the gas phase has been designed and fabricated. It combines supersonic jet expansion technique with fluorescence and mass detection methods to carry out IR–UV double resonance spectroscopic measurements. The fluorescence-detected infrared spectra of phenylacetylene and phenylacetylene–argon complex reveal that the π-bound argon acts as a perfect messenger to probe the acetylenic C–H stretching vibration of the phenylacetylene moiety in S_0 and S_1 states. The rare gas tagging method along with the infrared pre-dissociation technique revealed that the spectrum of phenylacetylene cation consists of two transitions, one of which can be assigned to the hot band and the other to acetylenic C–H stretching vibration of phenylacetylene. We have demonstrated that the difference in the internal cooling between argon and neon tagging can be used as a tool to assign hot bands.

Keywords: Double resonance spectroscopy, laser induced fluorescence, molecular clusters, resonant two photon ionization.

RARE gas clusters have been a subject of interest because of their role in understanding intermolecular interactions[1–3]. Over the last two decades, the combination of laser spectroscopy and molecular beam techniques has contributed to achieve more insights on intermolecular interactions at an unprecedented microscopic level. The versatile supersonic jets and beams technique can be used to produce clusters which are molecular entities bound by weak intermolecular interactions, such as van der Waals forces or hydrogen bonding, by co-expansion of the required reagents. Molecular clusters produced under cold and isolated condition of supersonic jets allow us to probe structures, intermolecular potentials and dynamics at a microscopic level with the aid of various laser spectroscopic techniques. Much of the earlier work on molecular clusters was carried out using electronic spectroscopy[4]. Electronic spectra of clusters exhibit characteristic spectral shifts depending on their size and/or structural differences, but do not give any structural information. Infrared (IR) spectroscopy along with various other spectroscopic techniques, such as NMR, has long been realized as an excellent technique to investigate local interactions present in molecules and molecular assemblies. However, IR spectroscopy in the gas phase, especially in supersonic jets and beams, cannot be achieved with conventional absorption measurements due to very low density. Further, selectivity is lost due to the presence of heavy mixture of undesired monomers and clusters along with the cluster/monomer of interest. In this respect, any spectroscopic technique to be used for the investigation of molecular clusters requires merits of having high sensitivity and selectivity. Lee and co-workers first demonstrated the IR spectroscopy of clusters by population labelling of target species using electronic transition, which enables the size/structure selection[5]. Brutschy and co-workers applied this for the first time to investigate fluorobenzene–methanol clusters, wherein they observed the C–O stretching vibration of methanol[6]. Later this technique has been popularized by Mikami's and Zwier's groups simultaneously, to investigate hydrogen bonding in phenol–water and benzene–water clusters respectively[7,8].

The infrared spectra of argon (Ar) complexes of several aromatic molecules, such as benzene[5,9], aniline[10], phenol[11], have been reported in the literature. In comparison with bare molecules those spectra are almost unperturbed. On the other hand, it has been amply demonstrated that Ar-tagging significantly reduces the internal temperatures of the cluster ions, without affecting the structure of the parent cluster[12–14]. These results form the basis for the 'messenger' technique[15–18]. However, in a few instances it has been observed that under some conditions Ar binding does affect the vibrational structure. For instance, it has been shown that in phenol and the series of fluorophenols, Ar binding in the cationic state leads to lowering of the O–H stretching vibration, which can be interpreted as formation of charge-assisted ionic O–H···Ar hydrogen bond[19,20]. On the other hand, the ability of neon tagging has not been explored, though it can be expected that neon would not be as effective as argon. In this article, we present the investigations carried out on phenylacety-

*For correspondence. (e-mail: naresh@chem.iitb.ac.in)

lene (PHA) and its argon complex in the neutral ground (S_0), neutral first excited (S_1), and the cationic (D_0) states probed using double resonance spectroscopic techniques. Further, we also demonstrate that the difference in the ability of internal cooling of neon and argon can be used to assign the hot bands.

Experimental

Design and working of the spectrometer

We have recently set up a spectrometer to investigate molecules and molecular clusters in the gas phase using double-resonance spectroscopic technique. The spectrometer combines the supersonic nozzle, which produces a cold jet of molecules, with fluorescence and ion detection systems. It consists of two cylindrical stainless steel (SS-304) chambers of size 250 mm–400 mm and 225 mm–150 mm, respectively, wherein the first dimension is height and second, the diameter. The two chambers are connected by a 650 mm long and 100 mm diameter stainless steel tube. The bigger chamber is pumped with a 3000 l/s oil diffusion pump (OD250; Hind Hivac) backed with 30 m^3/h rotary vane pump (ED30; Hind Hivac), while the smaller chamber is connected to a 700 l/s diffstack diffusion pump (700M; Edwards) backed by the 12 m^3/h rotary vane pump (2012; Alcatel). To prevent back-streaming of the diffusion pump oil, the bigger chamber is fitted with a custom-designed cold water baffle. Further, both the chambers are fitted with appropriate gate valves, which can be used to isolate the chambers from the oil diffusion pumps, if necessary. In order to achieve good pumping rates for the oil diffusion pumps and to reduce back-streaming, the highest grade diffusion pump oil (Santovac-5; Varian) has been used. Typical base pressure in the entire vacuum system is about 5×10^{-7} torr. The bigger chamber consists of four ports at right angles, two of which are used for guiding the lasers into the chamber. The third port is fitted with the fluorescence detection system along with the electrostatic grids for the time-of-flight mass spectrometer (TOFMS). The fourth port is used to connect the long tube which serves as a flight tube for the TOFMS. The pulsed nozzle is guided into the bigger chamber with the help of a stainless steel tube fitted with a sample holder. The sample holder and the pulsed nozzle can be heated up to 200°C, which facilitates investigating compounds which have low vapour pressures under ambient conditions.

The spectrometer has the advantage of detecting fluorescence and mass signals simultaneously in one set-up. A seeded supersonic free-jet is produced by co-expansion of the desired reagent in a buffer gas held at a high pressure (typically 3–5 atm) through a 200 μm diameter pulsed nozzle (Series-9; General Valve Corporation), driven by a pulsed valve driver (Iota One; General Valve Corporation) into a high-vacuum chamber. The pulsed valve driver works at a frequency of 10 Hz, with a typical on time of 120–150 μs, corresponding to a duty cycle of 0.15% and the resulting ambient pressure is about 1×10^{-5} torr. The excitation laser intersects the gas pulse at right angles 10 mm downstream from the nozzle. The ensuing fluorescence is collected perpendicular to both gas and laser pulses using 50 mm focal length *f/1* lens. Only a single *f/1* lens is used in the entire collection set-up to avoid reflection losses. The distance of the *f/1* lens from the object (the interaction region of the jet and the laser) is adjusted such that the image of the fluorescence from the jet is focused on the photocathode of the PMT. Total florescence is detected using a photomultiplier tube (PMT – 9780SB+ 1252-5F; Electron Tubes Limited)/filter (WG305+BG3, Astro Optical Industries) combination.

Alternatively, mass detection can also be done using the TOFMS, which is based on the Wiley–McLaren design[21]. It consists of three 50 mm grids, the repeller (R), extractor (E) and accelerator (A) and 1.1 m field-free flight tube. The distance between R and E is 2.5 cm and the distance between E and A is 1 cm. The interaction region between the gas and the laser beams is midway between the R and E grids, perpendicular to the direction of the TOFMS. The ions are extracted by high-voltage electric fields. Typically, voltages of +3000 and +1700 V are applied to the R and E grids, respectively, and A is grounded. The ions produced are extracted out of the ionization region by an electric field of 520 V cm^{-1} and are accelerated by an electric field of strength 1800 V cm^{-1}. The accelerated ions enter the field-free region of length 1.1 m to reach the channel electron multiplier (CEM-KBL-25RS; Sjuts) operated typically around –1800 V. A Faraday cup is used to collect the electrons, through a filter circuit biased at +250 V and processed with a broadband preamplifier (EG&G PARC, Model 115). The signal from the PMT/CEM is digitized by a digital storage oscilloscope (TDS-1012; Tektronix), which is interfaced to a PC via the PCI-GPIB card. The waveforms are integrated and averaged utilizing a data acquisition program written using LabView. The integrated signal is plotted against the wavelength to get the fluorescence/R2PI spectrum.

Spectroscopic techniques

Three different experimental techniques have been used for complete spectroscopic identification and characterization of bare molecules and molecular clusters in supersonic jets[22]. As mentioned earlier, the much-required selectivity of the neutral clusters is provided by electronic transitions, which can be monitored using either fluorescence and/or resonantly enhanced multiphoton ionization (REMPI) induced by an ultraviolet (UV) laser[5–8]. The combined technique is called IR–UV double resonance spectroscopy, and has been applied to various neutral

clusters, as long as they show a distinct sharp transition in their $S_1 \leftarrow S_0$ electronic spectrum. In this technique a pulsed UV laser excites the origin band of the $S_1 \leftarrow S_0$ transition and the ensuing fluorescence or REMPI signal is monitored as a measure of the ground-state population. Prior to the UV laser an IR laser is introduced and its wavelength is scanned. When the IR wavelength is resonant with a vibrational transition of the species, the IR absorption induces reduction of the population, which is then detected as a decrease in the fluorescence or REMPI signal intensity. The resultant spectrum is called fluorescence detected IR (FDIR) or ion detected IR (IDIR) spectrum depending upon the detection scheme used. In the electronic excited state an alternative method called UV–IR double resonance spectroscopy is used, which is just a time-inverted method of the IR–UV spectroscopic technique. In this method, an UV laser prepares the molecules in the zeroth vibrational level of the S_1 state. An IR pulse, introduced following the UV pulse within the radiative lifetime of the S_1 state, pumps the molecules to higher vibrational levels in the S_1 state. For most of the molecules the fluorescence quantum yield decreases with the higher vibrational energy in the S_1 state. When the IR wavelength is resonant with a vibrational transition of the species in the S_1 state, the IR absorption leads to a reduction of the quantum yield, which is then detected as a decrease in the fluorescence intensity. Only the fluorescence detection method is suitable for this technique. To record the IR spectra in the cationic state, infrared pre-dissociation (IRPD) spectroscopic technique is used for molecular clusters. In this technique, the cluster cations are produced via REMPI using and UV pulse. The IR laser pulse is delayed relative to the UV pulse, typically about 10 ns, and scanned. When the IR wavelength is resonant on vibrational transitions of the cluster ion, the vibrational excitation leads to vibrational pre-dissociation of the parent cluster ion, leading to the production of fragment cations and lowering of the parent ion signal. The IR spectrum is thus detected by monitoring the loss of the parent ion signal.

Lasers

In order to perform the double resonance spectroscopic experiments, UV and IR laser sources are required. The UV source is a frequency-doubled output of a tunable dye laser (Radiant Dyes, Narrow Scan GR) pumped with second harmonic of a Nd : YAG laser (Continuum, Surelite I-10). On the other hand, the tunable IR source is an idler output of a $LiNbO_3$ optical parametric oscillator (Euroscan Instruments, Custom $LiNbO_3$ OPO) pumped with an injection seeded-single mode Nd : YAG laser (Quantel, Brilliant B). The dye laser was calibrated using the optogalvanic method and the IR OPO was calibrated by measuring the wavelength of red light (~645 nm) generated by the sum frequency of signal and pump beams using a standardized monochromator (Spex 0.3 m). The absolute frequency calibration is within ± 3 cm^{-1}. The typical bandwidth of both UV and IR lasers is about 1 cm^{-1}. The timing between the IR and UV lasers was controlled electronically with a digital delay pulse generator (DDG-555; Berkeley Nucleonics Corporation).

Results and discussion

Figure 1 shows the one colour-resonant two photon ionization (1C-R2PI) mass spectrum of the PHA–Ar system recorded using the excitation laser fixed at 35,846 cm^{-1}. Apart from PHA and PHA–Ar, the mass spectrum also consists of peaks due to PHA–water complex and PHA dimer. Figure 2 *a* shows the LIF spectrum of PHA recorded with argon as buffer gas. Figure 2 *b* and *c* also depict the 1C-R2PI spectra of PHA, and PHA–Ar complex respectively. The band-origin transitions of PHA and PHA–Ar complex are at 35,876 and 35,846 cm^{-1} respectively, and are in good agreement with those reported in the literature[23,24]. The origin band of the argon complex is shifted to the red by 30 cm^{-1} relative to the bare PHA and is comparable to that of the benzene–argon complex[25]. The 1C-R2PI spectrum of PHA–Ar complex also shows two low-frequency transitions at 15 and 41 cm^{-1} respectively relative to the band origin which can be assigned to the bend and stretch along the intermolecular coordinate[26].

The infrared spectra in the acetylenic C–H stretching region were recorded using double resonance technique. Figure 3 depicts the FDIR spectra of PHA and its argon complex in the S_0 and S_1 states. The FDIR spectrum of bare PHA (Figure 3 *a*) shows two intense transitions at

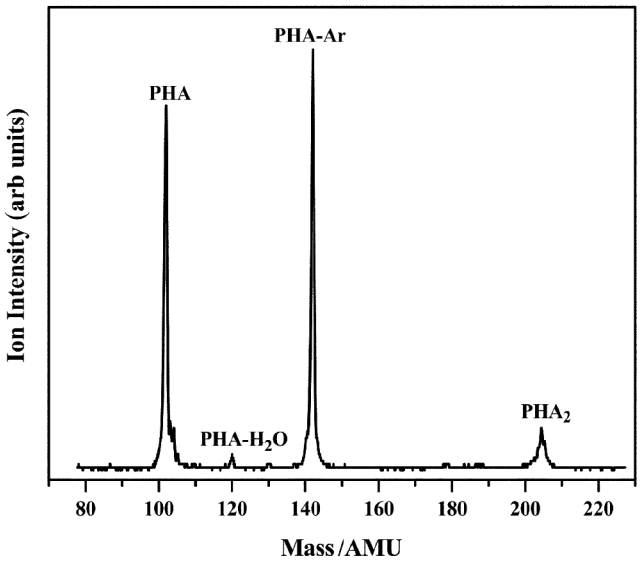

Figure 1. 1C-R2PI mass spectrum of phenylacetylene–argon system. The excitation laser was tuned to the band-origin transition of phenylacetylene–argon complex at 35,846 cm^{-1}.

3325 and 3343 cm^{-1} respectively, along with few weak transitions. The two intense transitions have been assigned to Fermi resonance bands between acetylenic C–H stretching vibration and a combination of one quantum of C≡C stretch and two quanta of C≡C–H out-of-plane bend[27]. Other weak features observed in the FDIR spectrum have been assigned to transitions arising out of higher order coupling terms[23,27]. The IR spectrum of the argon complex (Figure 3 *b*) is almost identical to that of the bare molecule, with the experimental uncertainty of ±1 cm^{-1}. This implies that the attachment of Ar to PHA does not perturb the acetylenic C–H oscillator. The FDIR spectra of PHA (Figure 3 *c*) and PHA–Ar complex (Figure 3 *d*) in the S_1 are almost identical. In these two spectra the lone transition at 3325 cm^{-1} can be assigned to the acetylenic C–H stretching vibration in the S_1 state.

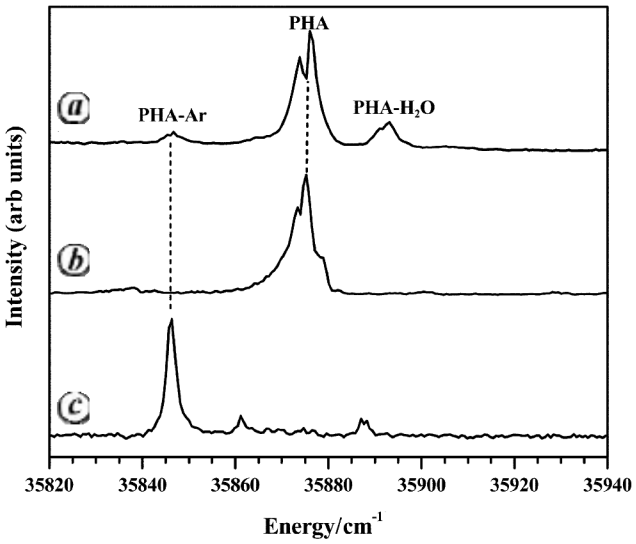

Figure 2. (*a*) LIF spectrum of phenylacetylene. 1C-R2PI spectrum of (*b*) phenylacetylene and (*c*) phenylacetylene–Ar. Spectra *a* and *c* were recorded using argon as buffer gas, while (*b*) was recorded using helium as buffer gas.

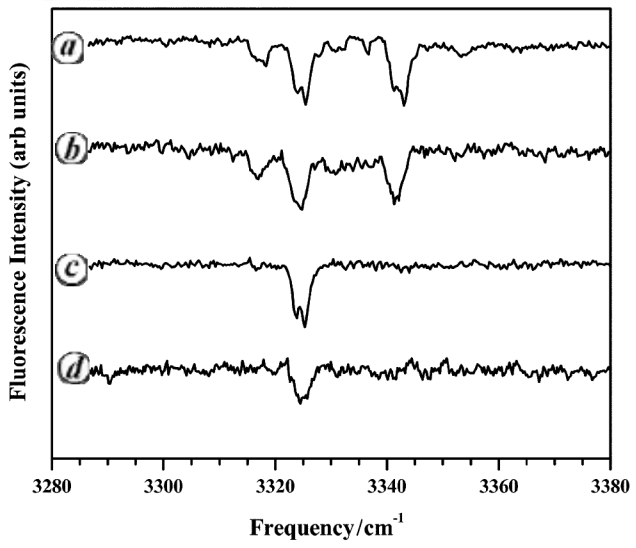

Figure 3. FDIR spectra of (*a*) phenylacetylene, (*b*) phenylacetylene–Ar in the S_0 state, (*c*) phenylacetylene, and (*d*) phenylacetylene–Ar in the S_1 state.

For a set of Fermi resonance bands with a separation of ΔE and intensity ratio of R, and assuming that the intrinsic (unperturbed) overtone intensity is negligible, the unperturbed separation ΔE_0 and the coupling matrix element W are given by[28,29]:

$$\Delta E_0 = \Delta E \cdot \frac{R-1}{R+1}, \tag{1}$$

$$W = \Delta E \cdot \frac{\sqrt{R}}{R+1}. \tag{2}$$

De-perturbation analysis was carried out for the 3325 and 3343 cm^{-1} peaks using eqs (1) and (2) with $R \approx 1.0$ and $\Delta E = 18$ cm^{-1}. We obtained values $\Delta E_0 \approx 0$ cm^{-1} and $W \approx 9$ cm^{-1}. (The average value of R obtained from ten scans of the IR spectra was 1.02 ± 0.05, hence we have used $R \approx 1$ for the de-perturbation analysis.) This implies that the energy difference between the zero-order vibrational states corresponding to the acetylenic C–H stretching vibration and the combination band of one quantum C≡C stretch and two quanta of C–H in-plane bend is within the bandwidth of the laser. Further, the stretching frequency of the unperturbed acetylenic C–H group can be estimated as 3334 cm^{-1}. This implies that upon electronic excitation the acetylenic C–H stretching vibration shifts to the red by 9 cm^{-1}.

The high-resolution REMPI spectrum for the $S_1 \leftarrow S_0$ electronic transition of the PHA–Ar complex was simultaneously fitted with the rotational constants for the ground and excited states[30]. The equilibrium structure consists of Ar atom bound to the π electron density of the benzene ring with the shift in Ar atom towards the acetylene group. On the other hand, Dreizler *et al.*[31] measured the microwave spectra of 24 isotopomers of the PHA–Ar complex. Along with high level *ab-initio* calculations carried out at CCSD(T)/CBS, these authors concluded that the Ar atom is placed over the benzene ring. However, there is substantial motion over the benzene ring to predict the exact position of the Ar arom[31]. The near identical IR spectra of PHA and PHA–Ar complex in the acetylenic C–H stretching region, as depicted in Figure 3, indicates that the binding of Ar to PHA does not perturb the acetylenic C–H oscillator, both in the S_0 and S_1 states. Since the Fermi resonance transitions in the S_0 state involve the coupling of the acetylenic C–H stretching vibration and a combination of one quantum of C≡C stretch and two quanta of C≡C–H out-of-plane bend, the persistence of the Fermi resonance in the PHA–Ar complex clearly indicates that the Ar atom does not interact with the acetylenic moiety of PHA and is therefore expected to bind to

the π electron density of the benzene ring. The FDIR spectrum is consistent with the structure of the PHA–Ar complex predicted by high-resolution electronic spectroscopy and microwave spectroscopy[30,31]. The FDIR spectra depicted in Figure 3 indicate that the Ar atom bound to PHA acts as a perfect messenger to probe the vibrations of the acetylenic group of PHA. Extending this analogy to the cationic state, one would expect that the infrared spectrum of $[PHA–Ar]^+$ would mirror the infrared spectrum of $[PHA]^+$. Figure 4 *a* shows the IRPD spectrum of $[PHA–Ar]^+$ in the acetylenic stretching region, which consists of two bands around 3268 and 3276 cm^{-1} respectively. In order to assign the bands it is necessary to understand the origins of these two bands. To begin with, four distinct possibilities exist for the appearance of two bands in the IRPD spectrum of $[PHA–Ar]^+$. (i) Reappearance of Fermi resonance/anharmonic coupling similar to that observed in the S_0 state. (ii) Combination bands involving intermolecular modes over the acetylenic C–H stretching vibration. (iii) Hot bands due to the formation of internally hot $[PHA–Ar]^+$ following resonant two-photon ionization. (iv) Appearance of two distinct isomers of $[PHA–Ar]^+$ to two different π and σ complexes, similar to that observed in the case of $[phenol–Ar]^+$ using electron impact ionization, leading to formation of C–H···Ar hydrogen bond in the cation complex.

To resolve the above issues and to assign the two bands, we recorded the IRPD spectrum of $[PHA–Ne]^+$ complex cation. The rationale behind such an exercise was as follows. (i) In the case of reappearance of Fermi resonance/anharmonic resonance in the D_0 state, the IRPD spectrum of $[PHA–Ne]^+$ would be identical to that of $[PHA–Ar]^+$. This is due to the fact that the π-bound Ar atom does not perturb the acetylenic C–H stretching vibration. Therefore, the π-bound Ne atom is not expected to make any difference, as the binding of Ne is weaker than that of Ar. (ii) Since the frequencies of the intermolecular vibrations would change upon the binding potential energy, it is expected that the positions of the combination bands of the neon complex would be different compared to the argon complex. (iii) In the instance of observation of a hot band, replacement of Ar with Ne would result in an increase in the intensity of the lower energy band, without change in the band positions. Such an observation can be attributed to the reduced efficiency of internal cooling of Ne relative to Ar. (iv) Finally, if the two peaks are due to π and σ complexes of $[PHA–Ar]^+$, the low frequency band which can be probably assigned to the σ complexes, resulting in C–H···Ar hydrogen bond cation complex would disappear completely, as the ability of neon to form C–H···Ne hydrogen bond would be much less in comparison with argon. Comparison of IRPD spectra of $[PHA–Ar]^+$ and $[PHA–Ne]^+$ should correspond to one of the four possibilities listed above. The IRPD spectrum of $[PHA–Ne]^+$ is shown in Figure 4 *b*. This spectrum clearly shows that the intensity of the lower frequency band at 3268 cm^{-1} is about 25% higher than the corresponding band in the spectrum of the argon complex. Based on the analysis presented above, the 3268 cm^{-1} transition can be unambiguously assigned to the hot band. Therefore, the 3276 cm^{-1} band can now be assigned to the acetylenic C–H stretching vibration in $[PHA–Ar]^+$ and $[PHA–Ne]^+$. Extending the analogy observed for the S_0 and S_1 states to the D_0 state, the acetylenic C–H stretching vibration of the phenylacetylene cation $[PHA^+]$ can be pegged at 3276 cm^{-1}.

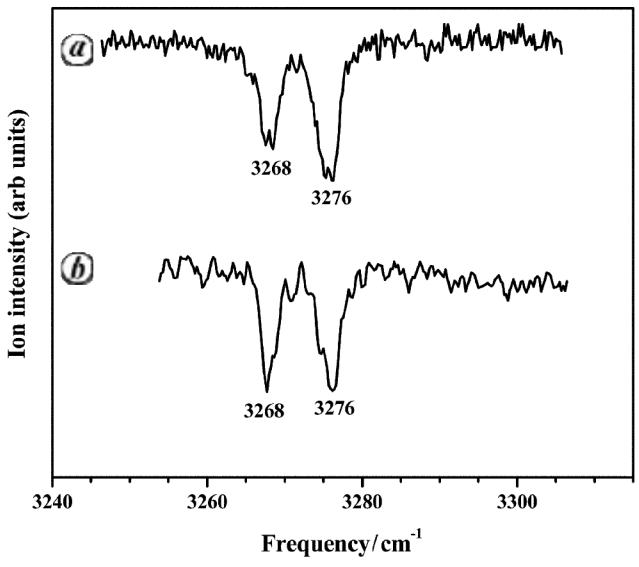

Figure 4. IRPD spectrum of (*a*) phenylacetylene–Ar and (*b*) phenylacetylene–Ne complex cations.

Conclusion

The IR spectra of PHA and its Ar complex were recorded in the acetylenic C–H stretching region using double resonance technique in the S_0, S_1 and D_0 states. In the S_0 state, the acetylenic C–H stretching vibration is involved in a Fermi resonance with the combination band of two quanta of out-of-plane C≡C–H bend and one quantum of C≡C stretch. The deperturbation analysis places the C–H stretching vibration at 3334 cm^{-1} in the S_0 state. In the S_1 state the corresponding frequency is 3325 cm^{-1}, a shift of –9 cm^{-1} relative to the S_0 state. The IRPD spectrum of phenylacetylene–argon cation complex shows two transitions at 3268 cm^{-1} and 3276 cm^{-1} respectively. Comparison of the relative intensities of the two transitions with those in the IRPD spectrum of phenylacetylene–neon cation complex reveals that the transition at 3268 cm^{-1} corresponds to a hot band, while the transition at 3276 cm^{-1} is the acetylenic C–H stretching vibration of the PHA^+ moiety. Thus the differences in the internal cooling due to argon and neon tagging can be a useful tool to understand and assign hot bands.

1. Neusser, H. J. and Siglow, K., High-resolution ultraviolet spectroscopy of neutral and ionic clusters: Hydrogen bonding and the external heavy atom effect. *Chem. Rev.*, 2000, **100**, 3921–3942.
2. Leutwyler, S. and Bosiger, J., Rare-gas solvent clusters: Spectra, structures, and order–disorder transitions. *Chem. Rev.*, 1990, **90**, 489–507.
3. Koch, H., Fernandez, B. and Christiansen, O., The benzene–argon complex: A ground and excited state *ab-initio* study. *J. Chem. Phys.*, 1998, **108**, 2784–2790.
4. Ito, M., Supersonic jet spectroscopy for the study of hydrogen bonding. *J. Mol. Struct.*, 1988, **177**, 173–190.
5. Page, R. H., Shen, Y. R. and Lee, Y. T., Infrared–ultraviolet double resonance studies of benzene molecules in a supersonic beam. *J. Chem. Phys.*, 1988, **88**, 5362–5376.
6. Riehn, C., Lahmann, C., Wassermann, B. and Brutschy, B., IR depletion spectroscopy. A method for characterizing a microsolvation environment. *Chem. Phys. Lett.*, 1992, **197**, 443–450.
7. Tanabe, S., Ebata, T., Fujii, M. and Mikami, N., OH stretching vibrations of phenol-$(H_2O)_n$ (n = 1–3) complexes observed by IR–UV double-resonance spectroscopy. *Chem. Phys. Lett.*, 1993, **215**, 347–352.
8. Pribble, R. N. and Zwier, T. S., Size-specific infrared spectra of benzene-$(H_2O)_n$ clusters (n = 1 through 7): Evidence for noncyclic $(H_2O)_n$ structures. *Science*, 1994, **265**, 75–79.
9. Venturo, V. A, Maxton, P. M. and Felker, P. M., Raman/vibronic double-resonance spectroscopy of benzene-doped argon clusters. *Chem. Phys. Lett.*, 1992, **198**, 628–636.
10. Nakanaga, T., Ito, F., Miyawaki, J., Sugawara, L. and Takeo, H., Observation of the infrared spectra of the NH_2-stretching vibration modes of aniline$\cdots Ar_n$(n = 1, 2) clusters in a supersonic jet using REMPI. *Chem. Phys. Lett.*, 1996, **261**, 414–420.
11. Fujii, A., Miyazaki, M., Ebata, T. and Mikami, N., Infrared spectroscopy of the phenol–N_2 cluster in S_0 and D_0: Direct evidence of the in-plane structure of the cluster. *J. Chem. Phys.*, 1999, **110**, 11125–11128.
12. Vaden, T. D., Forinash, B. and Lisy, J. M., Rotational structure in the asymmetric OH stretch of $Cs^+(H_2O)Ar$. *J. Chem. Phys.*, 2002, **117**, 4628–4631.
13. Ayote, P., Bailey, C. J., Kim, J. and Johnson, M. A., Vibrational predissociation spectroscopy of the $(H_2O)_6^-\cdot Ar_n$, $n \geq 6$, clusters. *J. Chem. Phys.*, 1998, **108**, 444–449.
14. Ayotte, P., Weddle, G. H., Kim, J. and Johnson, M. A., Vibrational spectroscopy of the ionic hydrogen bond: Fermi resonances and ion–molecule stretching frequencies in the binary $X^-\cdot H_2O$ (X = Cl, Br, I) complexes via argon predissociation spectroscopy. *J. Am. Chem. Soc.*, 1998, **120**, 12361–12362.
15. Okumura, M., Yeh, L. I., Myers, J. D. and Lee, Y. T., Infrared spectra of the cluster ions $H_7O_3^+\cdot H_2$ and $H_9O_4^+\cdot H_2$. *J. Chem. Phys.*, 1986, **85**, 2328–2329.
16. Okumura, M., Yeh, L. I., Myers, J. D. and Lee, Y. T., Infrared spectra of the solvated hydronium ion: Vibrational predissociation spectroscopy of mass-selected $H_3O^+\cdot(H_2O)n\cdot(H_2)_m$. *J. Phys. Chem.*, 1990, **94**, 3416–3427.
17. Boo, D. W. and Lee, Y. T., Infrared spectroscopy of the molecular hydrogen solvated carbonium ions, $CH_5^+(H_2)_n$ (n = 1–6). *J. Chem. Phys.*, 1995, **103**, 520–530.
18. Fujii, A., Fujimaki, E., Ebata, T. and Mikami, N., Infrared spectroscopy of CH stretching vibrations of jet-cooled alkylbenzene cations by using the 'messenger' technique. *J. Chem. Phys.*, 2000, **112**, 6275–6284.
19. Solca, N. and Dopfer, O., IR spectra of para-substituted phenol$^+$–Ar cations: Effect of halogenation on the intermolecular potential and O–H bond strength. *Chem. Phys. Lett.*, 2003, **369**, 68–74.
20. Solca, N. and Dopfer, O., Infrared spectra of the H-bound and π-bound isomers of the phenol–argon cation. *J. Mol. Struct.*, 2001, **563–564**, 241–244.
21. Wiley, W. C. and McLaren, I. H., Time-of-flight mass spectrometer with improved resolution. *Rev. Sci. Instrum.*, 1955, **26**, 1150–1157.
22. Fujii, A., Patwari, G. N., Ebata, T. and Mikam, N., Vibrational spectroscopic evidence of unconventional hydrogen bonds. *Int. J. Mass Spectr.*, 2002, **220**, 289–312.
23. King, G. W. and So, S. P., Ethynylbenzene analysis of the 2790 Å absorption system. *J. Mol. Spectrosc.*, 1971, **37**, 543–570.
24. Dao, P. D, Morgan, S. and Castleman Jr, A. W., Resonance-enhanced multiphoton ionization of van der Waals molecules: Studies of spectroscopic shifts of phenylacetylene clustered with molecules and atoms. *Chem. Phys. Lett.*, 1984, **111**, 38–46.
25. Schmidt, M., Calve, J. L. and Mons, M., Structural transitions in benzene–argon clusters: Size and temperature effects. *J. Chem. Phys.*, 1993, **98**, 6102–6120.
26. Meenakshi, P. S., Biswas, N., Patwari, G. N. and Wategaonkar, S., Vibrational predissociation in aminophenol–$argon_1$ complex. *Chem. Phys. Lett.*, 2003, **369**, 419–427.
27. Stearns, J. S. and Zwier, T. S., Infrared and ultraviolet spectroscopy of jet-cooled *ortho*-, *meta*-, and *para*-diethynylbenzene. *J. Phys. Chem. A*, 2003, **107**, 10717–10724.
28. Herzberg, G., *Infrared and Raman Spectra of Polyatomic Molecules*, Van Nostrand, New York, 1945.
29. Daunt, S. J. and Shurvell, H. F., The gas phase infrared band contours of s-triazine and s-triazine-d_3: The fundamentals of $C_3N_3H_3$ and $C_3N_3D_3$ and some overtone and combination bands of $C_3N_3H_3$. *J. Mol. Spectrosc.*, 1976, **62**, 373–395.
30. Siglow, K. and Neusser, H. J., Rotationally resolved UV spectroscopy of weakly bound complexes: Structure and van der Waals vibronic bands of phenylacetylene–Ar. *Chem. Phys. Lett.*, 2001, **343**, 475–478.
31. Dreizler, H., Hartke, B. and Rudolph, H. D., A contribution to the structure of the van der Waals complex phenylacetylene–argon by microwave spectroscopy and quantum chemistry. *J. Mol. Struct.*, 2006, **825**, 1–19.

ACKNOWLEDGEMENTS. This study was supported by the Department of Science and Technology, Board of Research in Nuclear Sciences, and Council of Industrial and Scientific Research, New Delhi. P.C.S. thanks CSIR for the award of senior research fellowship.

Received 9 February 2008; revised accepted 16 July 2008